

Advances in Geosciences
Vol. 21: Solar & Terrestrial Science (2008)
Ed. Marc Duldig
© World Scientific Publishing Company

IONOSPHERIC OBSERVATION USING FM-CW RADAR ARRAY

A. IKEDA*, A. YOSHIKAWA and M. G. CARDINAL

*Department of Earth and Planetary Sciences,
Kyushu University, Japan
a-ikeda@geo.kyushu-u.ac.jp

K. YUMOTO

*Space Environment Research Center,
Kyushu University, Japan*

M. SHINOHARA

Kagoshima National College of Technology, Japan

K. NOZAKI

*National Institute of Information and
Communications Technology, Japan*

B. M. SHEVTSOV and V. V. BYCHKOV

*Institute of Cosmophysical Research and Radiowaves
Propagation of the Far Eastern Branch of Russian
Academy of Sciences, Russia*

Q. M. SUGON, Jr. and D. McNAMARA

Manila Observatory, Philippines

In order to understand the electro-magnetic phenomena in space, the Space Environment Research Center (SERC) of Kyushu University is deploying the MAGnetic Data Acquisition System of the Circum-pan Pacific Magnetometer Network (MAGDAS/CPMN). In this network, we also installed FM-CW (Frequency Modulated Continuous Wave) radars at Paratunka, Russia (PTK: Magnetic Latitude = 45.8° , Magnetic Longitude = 221.6°), Sasaguri, Japan (SAS: M. Lat. = 23.2° , M. Lon. = 199.6°), and Manila, Philippines (MNL: M. Lat. = 4.19° , M. Lon. = 192.4°) to detect the ionospheric electric field variations. The FM-CW radar is a kind of HF (High Frequency) radar that can measure the ionospheric Doppler velocity, from which we can calculate the ionospheric electric fields. In the present paper we will introduce our FM-CW radar array observations and its preliminary scientific results. The results are as follows: (1) At the time of SC, dusk-to-dawn and subsequent dawn-to-dusk electric field penetrate into the low-latitude ionosphere. (2) Pi 2-associated

ionospheric electric field at $L = 2.05$ is a manifestation of the plasmaspheric cavity mode. (3) Ground Pc 5 pulsation seems to be driven by ionospheric electric field at low and equatorial region.

1. Introduction

The Space Environment Research Center (SERC) of Kyushu University in Fukuoka, Japan is deploying a magnetic observation array, which is called the MAGnetic Data Acquisition System of the Circum-pan Pacific Magnetometer Network (MAGDAS/CPMN).¹⁻³ In this network, we also initiated the installation of FM-CW (Frequency Modulated Continuous Wave) radars to measure the ionospheric electric fields. An FM-CW radar is a kind of HF (High Frequency) radar that can detect Doppler velocity of a target for ionospheric observation.⁴

The magnetic field measured on the ground is a superposition of various internal and external sources. The external sources are the solar wind, the magnetosphere, and the ionosphere. Among these sources, FM-CW radar observation provides only the information from the ionosphere. Therefore an analysis that combines the data from the MAGDAS/CPMN and FM-CW radars is expected to give us a better understanding of magnetospheric and ionospheric phenomena from the ground observations. For example, one benefit of combining ionospheric electric field data and magnetic field data is to allow us to identify the propagation modes of geomagnetic pulsations.

It is known that HF Doppler measurements at low- and mid-latitudes often show a good correlation with the variations of geomagnetic phenomena (e.g. Ref. [5]). For example, SCs (e.g. Refs. [6, 7]), Pc 5 pulsations (e.g. Refs. [8, 9]), Pc 3-4 pulsations (e.g. Refs. [10, 11]), and Pi 2 pulsations (e.g. Refs. [12, 13]) were reported using HF Doppler measurements. However, the comparison analysis of ionospheric response and ground magnetic field is limited. In this paper, we introduce our FM-CW radar observation and show some geomagnetic phenomenon observed simultaneously by the FM-CW radars and magnetometers of MAGDAS/CPMN.

2. Observation and Instruments

We installed FM-CW (Frequency Modulated Continuous Wave) radars at Paratunka, Russia (PTK: Magnetic Latitude = 45.8° , Magnetic Longitude

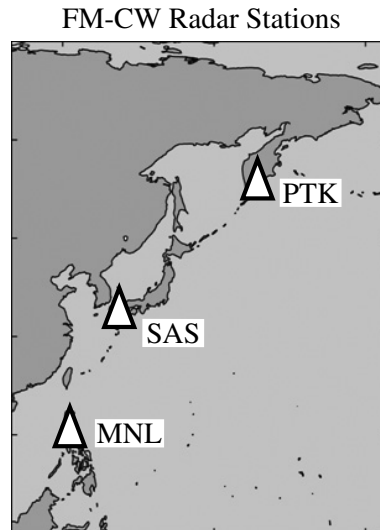


Fig. 1. Station map of FM-CW radars. The three stations are located at PTK, Russia, SAS, Japan, and MNL, Philippines.

= 221.6° , LT = UT + 10.5 hrs), Sasaguri, Japan (SAS: M. Lat. = 23.2° , M. Lon. = 199.6° , LT = UT + 9.5 hrs) and Manila, Philippines (MNL: M. Lat. = 4.19° , M. Lon. = 192.4° , LT = UT + 8.5 hrs). Figure 1 shows a station map of the currently installed FM-CW radars. They are located almost in the same longitude. The FM-CW radars at SAS and PTK were installed in 2000 and 2005, respectively. The latest installation was done on March 2009 at MNL. Figure 2 shows the FM-CW radar system at Manila, Philippines and Fig. 3 shows the tower for the radar. The FM-CW radar system consists of a receiver, a transmitter, and a control PC (from left). The PC controls the FM-CW radar and sends observational data to SERC via internet. The radar tower at MNL is a 100-foot tower with a dipole antenna mounted on top of it.

An FM-CW radar is a type of HF radar that can measure the range of target as well as its Doppler information. Our radar is an improved version of the FM-CW radar developed by Nozaki and Kikuchi.^{14,15} Poole¹⁶ and Poole and Evance¹⁷ used FM-CW radar for ionospheric Doppler measurement for the first time. Our Doppler observation is based on the fast Fourier transform (FFT) method which is a variation of a technique developed by Barrick¹⁸ to measure ocean waves. This technique provides

FM-CW Radar System at Manila

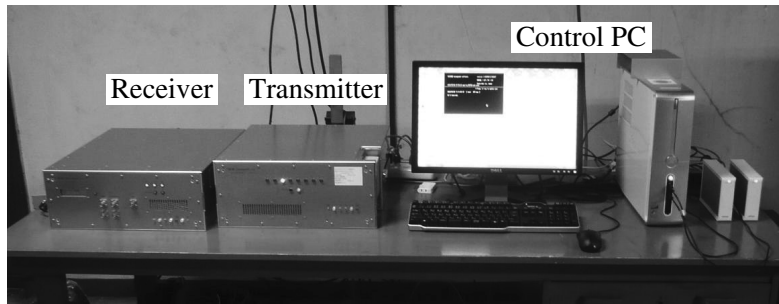


Fig. 2. FM-CW radar system at MNL. The components are a receiver, a transmitter, and a control PC (from left).

FM-CW Radar Tower at Manila

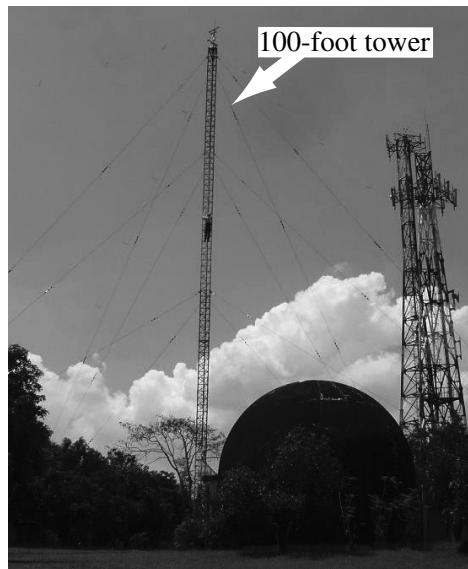


Fig. 3. A tower of FM-CW radar at MNL. The length of the tower is 30 foot. A dipole antenna is set to the tower.

us the Doppler velocity of a target and its distance. Generally FM-CW radars sweep their transmitting frequency slightly (e.g. from 3.00 MHz to 3.01 MHz) for Doppler observation and transmit signals continuously. In the FFT method, range and Doppler information can be estimated using a

double FFT. The first FFT over each sweep yields the range information, and the second FFT for each range bin over a number of sweeps provides the Doppler frequency. For our observation, the sweep rate is 200 or 100 kHz/sec and sweep time is 0.1 seconds. The observed Doppler frequency Δf is represented by

$$\Delta f = f_0 \times 2V^*/c \quad (1)$$

where f_0 is the transmitting frequency and V^* is vertical drift velocity of the ionosphere describe by

$$V^* = c \times \Delta f / 2f_0 \quad (2)$$

We use low frequency (e.g. 2.5 MHz) for the transmitting frequency f_0 at night and we use higher frequency (e.g. 5.0 MHz) at daytime. The data of Doppler velocity is digitized with 3-sec or 10-sec sampling. The data accuracy of the vertical drift velocity is 3.9 m/s at 3.0 MHz.

By assuming that the V^* is caused by the frozen-in effects in the ionosphere, we can estimate the east-west ward electric field (E_y). The equation of the frozen-in effect is described

$$\mathbf{E} = -\mathbf{V} \times \mathbf{B} \quad (3)$$

where \mathbf{E} is east-west electric field (E_y), and \mathbf{B} is the horizontal component (H component) of the magnetic field in the ionosphere, and \mathbf{V} is obtained by FM-CW radars. A schematic diagram of the Doppler measurement by an FM-CW radar is shown in Fig. 4.

3. Observational Results and Discussion

3.1. Sudden commencement

Figure 5 shows the geomagnetic H component (H) at Kuju, Japan (KUJ: M. Lat. = 23.6°, M. Lon. = 203.2°, LT = UT + 8.7 hrs) and the ionospheric electric field E_y at SAS on 4 November, 2003. The time interval is 10 minutes from 06:22 UT to 06:32 UT corresponding to the local daytime. During this SC event, the transmitting frequency f_0 was 8.0 MHz and the observed ionospheric altitude was about 260 km (virtual height). A time resolution of E_y and H for this event is 10 seconds, and 3 seconds, respectively. The E_y at SAS shows a small variation prior to the onset of the SC (described by the vertical dashed line in Fig. 5). At 06:25:45 UT (indicated by the black arrow), the E_y started to decrease within a few of

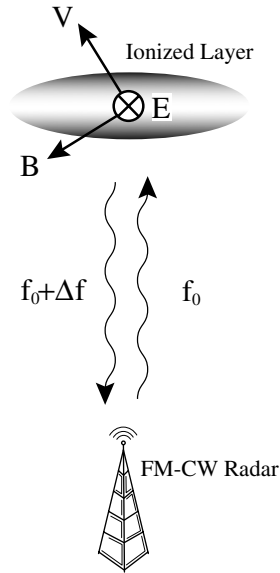


Fig. 4. Schematic diagram of the Doppler measurement of the ionosphere. When the eastward electric field penetrates into the low-latitude ionosphere, it drifts upward because of $\mathbf{E} \times \mathbf{B}$ drifts.

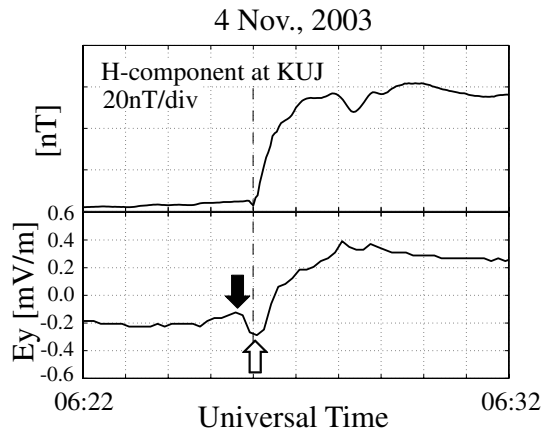


Fig. 5. SC at daytime on 4 November, 2003. The upper panel shows the ground H component at KUJ. The bottom panel shows the E_y at SAS, which is calculated from the observed ionospheric Doppler velocity. The transmitting frequency of the FM-CW radar was 8.0 MHz during this event.

tens seconds and reached the minimum value of -0.29 mV/m at 06:26:05 UT (indicated by the white arrow). The value was -0.15 mV/m (westward) and the duration was 30 seconds. This signature coincides with slightly negative variation of the H at KUJ which is the so-called PRI (preliminary reverse impulse). The PRI is well known that it often appears at the time of PI (Preliminary Impulse) in daytime low- and equatorial region.¹⁹ The westward electric field at the time of PRI corresponds to the dusk-to-dawn direction.

After the E_y attained its minimum value (indicated by the white arrow), it increased rapidly from -0.29 to 0.39 mV/m during a period from 06:26:05 UT to 06:28:05 UT. The amplitude of this increase is 0.68 mV/m (eastward). This eastward electric field corresponded with dawn-to-dusk electric field. In addition, the timing of the eastward electric field and increasing of H (so-called Main Impulse MI) was same.

The nighttime SC event is shown in Fig. 6. The format is the same as that of Fig. 5. The time interval is from 17:06 UT to 17:16 UT on 21 January, 2005. During this SC event, the FM-CW radar observed the altitude of about 360 km (virtual height) at 2.5 MHz. At 17:11:15 UT (indicated by the black arrow), the E_y showed a sudden increase from 0.0 mV/m to 0.26 mV/m within a few of tens of seconds. This eastward electric field preceded a sudden increase of the magnetic H component. Therefore it can be identified as a dusk-to-dawn electric field corresponding with daytime PRI.

At the time of MI onset indicated by the vertical dashed line in Fig. 6, the E_y decreased with increasing H almost simultaneously at 17:11:35 UT (indicated by the black arrow). The decrease of 1.16 mV/m in E_y indicates the existence of westward electric field. The direction is dawn-to-dusk.

It has been known that the interplanetary and magnetospheric electric field can penetrate into the low-latitude ionosphere (e.g. Ref. [19]). The IEF (Interplanetary Electric Field) can continuously penetrate to the low-latitude ionosphere without significant attenuation.²⁰ Short life time (<3 hours) dawn-dusk IEF penetrate into the ionosphere without shielding.²¹ Also penetration of electric fields has been reported in the case of SC (e.g. Refs. [6, 22]). Araki²³ concluded that the PI is caused by a dusk-to-dawn electric and the MI is caused by a dawn-to-dusk electric field. The two types of electric fields are generated in the magnetosphere by a solar wind pressure enhancement and penetrate into the polar ionosphere and low-latitude ionosphere. This is consistent with our result.

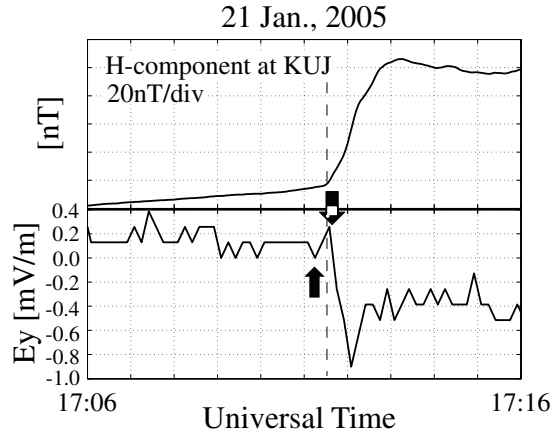


Fig. 6. SC at nighttime on 21 January 2005. The format is the same as that of Fig. 4. The transmitting frequency was 2.5 MHz during this event.

3.2. *Pi 2 pulsation*

Figure 7 shows a nighttime Pi 2 (40–150 seconds) event observed by an FM-CW radar and a MAGDAS magnetometer at PTK on 19 October 2007. During this event, the FM-CW radar observed the altitude of about 250 km (virtual height) at 3.0 MHz. The ground magnetic H and D components (D) obtained at PTK ($L = 2.05$, $LT = UT + 10.5$ hrs) and Ashibetsu, Japan (ASB; M. Lat. = 34.7° , M. Lon. = 209.6° , $L = 1.48$, $LT = UT + 9.5$ hrs), and E_y at PTK are plotted in Fig. 7. The E_y is 3-sec time resolution and the ground magnetic data is 1-sec time resolution for this event. The thick lines indicate H components and the thin lines indicates D components.

Figure 8 shows the band pass filtered data. We can see that Pi 2 pulsations were observed simultaneously in H and V^* . They started around 1644 UT and attained their peak around 16:48 UT (see the H component at PTK in Fig. 8). The dominant frequency was 15.4 mHz for all waves. Fig. 8 also shows the filtered H and D components at PTK and ASB, and the filtered E_y at PTK. The peak-to-peak amplitude of H at PTK, D at PTK, H at ASB, D at ASB, and E_y at PTK are 3.3 nT, 1.4 nT, 2.5 nT, 1.2 nT, and 0.43 mV/m, respectively. The ground magnetic perturbation was dominant at H components rather than at D components.

We calculated the cross correlation between E_y at PTK and geomagnetic field data. As a result, the maximum correlation coefficients were 0.95 for $E_y - H$ (PTK), 0.95 for $E_y - H$ (ASB), 0.79 for $E_y - D$

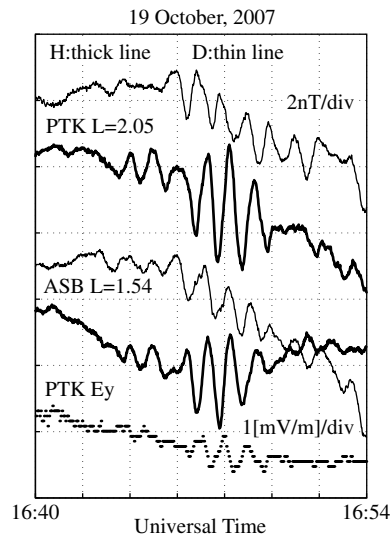


Fig. 7. Pi 2 pulsations on 19 October 2007. H and D components at PTK and ASB and E_y at PTK. The thick lines are H components and the thin lines are D components. The transmitting frequency of the FM-CW radar was 3.0 MHz.

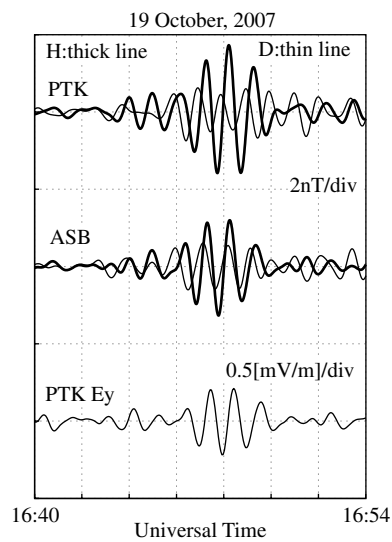


Fig. 8. Band pass filtered (40–150 seconds) H and D components at PTK and ASB and E_y at PTK on 19 October 2007. The thick lines are H components and the thin lines are D components for magnetic field data.

(PTK), 0.72 for $E_y - D$ (ASB). Thus the correlation coefficient of $E_y - H$ is higher than that of $E_y - D$. In addition, the correlation coefficient of $E_y - H$ (ASB) is higher than that of $E_y - H$ (PTK).

Pi 2 pulsations are well known as the signal for the onset of magnetic substorms (e.g. Ref. [24]). Moreover low-latitude Pi 2 pulsations are explained in terms of the plasmaspheric cavity mode (e.g. Ref. [25]). Takahashi *et al.*²⁶ analyzed the ground magnetic H component at KAK ($L = 1.26$) and the magnetic field variation obtained by AMPTE CCE inside the plasmasphere. They found that nighttime Pi 2 pulsations originated from a cavity-mode-type resonance excited in the inner magnetosphere. In addition, the magnetic field variations on Pi 2 pulsations in the ionosphere and on the ground given by Han *et al.*²⁷ were consistent with the radial cavity mode. They found that the Pi 2 waves observed at KAK and by the low-altitude satellite ($h = 638 - 849$ km) Ørsted were highly coherent and oscillated without phase lag at nighttime. They concluded that the nightside Pi 2 pulsations at low latitude are directly propagated from the magnetosphere to the ground and became the cavity-mode oscillation. Thus low-latitude Pi 2 pulsations in ground H components are explained in terms of the plasmaspheric cavity mode. On the basis of previous studies, it seems that our result also suggests that the ionospheric E_y at PTK ($L = 2.05$) is a manifestation of the plasmaspheric cavity mode because the Pi 2 pulsation in E_y shows high correlation coefficient with lower-latitude H components.

3.3. Pc 5 pulsation

The daytime Pc 5 pulsation (150–600 seconds) observed by an FM-CW radar at SAS are shown in Fig. 9. The H component at equatorial station YAP (M. Lat. = 0.42° , M. Lon. = 209.9° , $L = 1.00$, $LT = UT + 9.2$ hrs) and KUJ ($L = 1.19$, $LT = UT + 8.7$ hrs) and E_y at SAS are plotted in Fig. 9. A time resolution of E_y and H for this event is 10 seconds, and 3 seconds, respectively. YAP, SAS, and KUJ were located at the local dayside sectors. During this event, the FM-CW radar at SAS recorded an altitude of 300 km at 8.0 MHz. The peak-to-peak amplitude of E_y at SAS was about 1.0 mV/m. The magnetic Pc 5 pulsation at YAP was larger than that at KUJ. The peak-to-peak amplitude at YAP was more than 100 nT. This would be due to equatorial enhancement because of the high ionospheric conductivity in the equatorial region (e.g. Ref. [24]). Inspecting the vertical dashed lines in Fig. 9, the peaks of H at KUJ and YAP almost corresponds

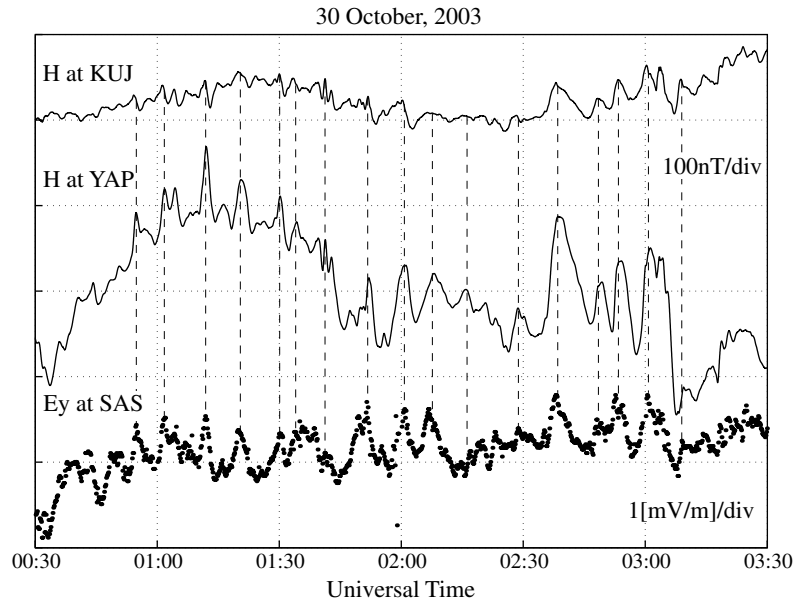


Fig. 9. Pc 5 pulsations on 31 October 2003. The ground magnetic H and D components at YAP and KUI and E_y at SAS are plotted. The FM-CW radar observed the altitude of about 300 km at 8.0 MHz.

with that of E_y at SAS. The positive peaks of E_y correspond with positive peaks of the H .

The oscillation of E_y at SAS corresponds with the H at KUI and YAP without significant time delay. This result suggests that the ground Pc 5 was excited by the ionospheric electric fields which drive ionospheric currents. The source of E_y for Pc 5 would be caused by the polar dawn-to-dusk electric fields which are excited by the DP 2 type current system.²⁸

4. Summary

In the MAGDAS/CPMN, SERC also deploys FM-CW radar observations to understand the Magnetosphere-Ionosphere phenomena in space. In this paper, we showed SC, Pi 2, Pc 5 events which were observed by MAGDAS/CPMN and FM-CW radars simultaneously. For these events, ionospheric perturbation correlated with ground magnetic field variation. In the future, we will study longitudinal structure of ionospheric electric fields

associated with geomagnetic phenomenon by using the FM-CW radars at PTK, SAS, and MNL.

Acknowledgment

We would like to thank Mr. Ryuichi Ishihara, Mr. Kazuhiro Mori, and Mr. Toshiki Shinbaru for helping to construct the FM-CW radar at Sasaguri, Japan. The FM-CW radar at Paratunka, Russia was installed with the support of the Institute of Cosmophysical Research and Radiowaves Propagation (IKIR) of the Far Eastern Branch of Russian Academy of Sciences. The FM-CW radar at Manila, Philippines was installed with the support of the Manila Observatory. We acknowledge all supporters for the FM-CW radar observation. We also acknowledge World Data Center for Geomagnetism, Kyoto (<http://wdc.kugi.kyoto-u.ac.jp/index.html>) for calculating the IGRF model.

References

1. K. Yumoto and the CPMN Group, *Earth Planets Space* **53** (2001) 981.
2. K. Yumoto and the MAGDAS Group, *Solar Influence on the Heliosphere and Earth's Environment: Recent Progress and Prospects* **309** (2006) 981.
3. K. Yumoto and the MAGDAS Group, *Bull. Astr. Soc. India* **35** (2007) 511.
4. A. Ikeda, K. Yumoto, M. Shinohara, K. Nozaki, A. Yoshikawa and A. Shinbori, *Mem. Fac. Sci., Kyushu Univ., Ser. D, Earth & Planet. Sci. Vol. XXXII* **1** (2007) 1.
5. K. L. Chan, D. P. Kanellakos and O. G. Villard Jr., *J. Geophys. Res.* **67** (1962) 2066.
6. T. Kikuchi, T. Ishimine and H. Sugiuchi, *J. Geophys. Res.* **90** (1985) 4389.
7. T. Araki, S. Fujitani, M. Emoto, K. Yumoto, K. Shiokawa, T. Ichinose, H. Luehr, D. Orr, D. Milling, H. Singer, G. Rostoker, S. Tsunomura, Y. Yamada and C. F. Liu, *J. Geophys. Res.* **102**(A7) (1997) 14075.
8. J. H. Sastri, K. B. Ramesh, D. R. K. Rao and J. V. S. V. Rao, *J. Atmos. Terr. Phys.* **55** (1993) 1271.
9. T. Motoba, T. Kikuchi, T. F. Shibata and K. Yumoto, *J. Geophys. Res.* **109**(A06214) (2004) doi:10.1029/2004JA010442.
10. R. A. Marshall and F. W. Menk, *Ann. Geophys.* **17** (1999) 1397.
11. F. W. Menk, *Planet. Space Sci.* **40** (1992) 495.
12. J. Klostermeyer and J. Röttger, *Planet. Space Sci.* **24** (1976) 1065.
13. J. F. Grant and K. D. Cole, *Planet. Space Sci.* **40** (1992) 1461.
14. K. Nozaki and T. Kikuchi, *Mem. Natl Inst. Polar Res., Spec. Iss.* **47** (1987) 217.
15. K. Nozaki and T. Kikuchi, *Proc. NIPR Symp. Upper Atm. Phys.* **1** (1988) 204.

16. A. W. V. Poole, *Radio Sci.* **20** (1985) 1609.
17. A. W. V. Poole and Evans, *Radio Sci.* **20** (1985) 1617.
18. D. E. Barrick, *NOAA Technical Report ERL*, **283-WPL** (1973) 26.
19. M. C. Kelley, J. J. Makela, J. L. Chau and M. J. Nicolls, *Geophys. Res. Lett.* **30**(4) (2003) 1158, doi:10.1029/2002GL016321.
20. C. -S. Huan, S. Sazykin, J. L. Chau, N. Maruyama and M. C. Kelley, *Atmos. Sol. Terr. Phys.* **69**(10–11) (2007) 1135.
21. Y. Wei, M. Hong, W. Wan, A. Du, J. Lei, B. Zhao, W. Wang, Z. Ren, and X. Yue, *Geophys. Res. Lett.* **35**(L02102) (2008), doi:10.1029/2007GL032305.
22. Y. -N. Huang, *J. Geophys. Res.* **81** (1976) 175.
23. T. Araki, *Geophysical Monograph 81* **183** (1994) 200.
24. T. Saito and S. Matsushita, *J. Geophys. Res.* **73** (1968) 267.
25. T. K. Yeoman and D. Orr, *Planet. Space Sci.* **38** (1989) 1367.
26. K. Takahashi, S. -I. Ohtani and B. J. Anderson, *J. Geophys. Res.* **100** (1995) 21929.
27. D. S. Han, T. Iyemori, M. Nose, H. McCreadie, Y. Gao, F. Yang, S. Yamashita and P. Stauning, *J. Geophys. Res.* **109**(A10209) (2004) 1210, doi:10.1029/2004JA010576.
28. T. Motoba, T. Kikuchi, H. Luhr, T.-I. Kitamura, H. Tachihara, K. Hayashi and T. Okuzawa, *J. Geophys. Res.* **107**(A2) (2002), doi:10.1029/2001JA900156.

May 10, 2010 13:50

AOGS - ST

9in x 6in

b951-v21-ch27